© 2025. This manuscript version is made available under the CC-BY-NC-ND 4.0 license https://creativecommons.org/licenses/by-nc-nd/4.0/
Accepted manuscript of: H. Li and J. Zhang, "Hydrogen's role in expanding renewable energy and reducing carbon emissions in Texas," International Journal of Hydrogen Energy, vol. 113, pp. 77-89, 2025. Published version: https://doi.org/10.1016/j.ijhydene.2025.02.303

Highlights

Hydrogen's Role in Expanding Renewable Energy and Reducing Carbon Emissions in Texas

Honglin Li,Jie Zhang

- **Hydrogen Integration**: Hydrogen enhances renewable energy penetration and reduces carbon emissions by balancing supply-demand mismatches in Texas.
- **Optimization Model**: A stochastic model optimizes hydrogen deployment, meeting up to 92.4% of hydrogen demand through strategic placement.
- **Emission Reductions**: Hydrogen integration and rising gas-fired electricity prices could cut 1,300 metric tons of CO2 annually by 2035.

Hydrogen's Role in Expanding Renewable Energy and Reducing Carbon Emissions in Texas

Honglin Li[a,b], Jie Zhang[a,b,c,*]

[a]Department of Mechanical Engineering, The University of Texas at Dallas, Richardson, 75080, TX, USA
[b]Center for Wind Energy, The University of Texas at Dallas, Richardson, 75080, TX, USA
[c]Department of Electrical and Computer Engineering, The University of Texas at Dallas, Richardson, 75080, TX, USA

ARTICLE INFO

Keywords:
Renewable energy
Hydrogen
Carbon emission reduction
Stochastic optimization

ABSTRACT

Texas, with its substantial wind and solar capacities, plays a pivotal role in the U.S. strategy to achieve net-zero emissions by 2050. Despite its leadership in wind energy generation and a growing solar sector, the integration of large-scale renewable energy in Texas faces significant challenges, primarily due to the intermittent nature of renewables and uncertainties surrounding future capacity expansion and demand growth. This study explores the potential of hydrogen as a solution to these challenges through a stochastic optimization model that accounts for the unpredictability of renewable energy installation timelines and fluctuations in electricity demand. The model designs a hydrogen network to mitigate geographical mismatches between energy supply and demand, providing a critical balancing mechanism. Our findings indicate that hydrogen can significantly enhance renewable energy penetration while reducing carbon emissions. Strategic placement of electrolyzers and hydrogen tanks, combined with inter-regional hydrogen transport, could satisfy up to 92.4% of hydrogen demand in certain regions. Additionally, annual hydrogen production across Electric Reliability Council of Texas (ERCOT) is projected to reach 131 tons, which corresponds to a carbon emissions reduction of 1,300 tons. Sensitivity analyses further reveal that higher electricity prices for combined cycle gas-turbine plants negatively impact the system's overall energy efficiency, leading to an increase in carbon emissions. For instance, when electricity prices rise to \$250 MWh^{-1}, annual system-wide carbon emissions increase by 310 kilotons compared to the benchmark scenario. This study highlights the critical role hydrogen can play in supporting Texas's renewable energy ambitions and underscores the necessity for policy backing, investment, and advancements in both hydrogen and carbon capture technologies to fully realize its potential.

1. Introduction

The international community has set ambitious goals for reducing carbon emissions and controlling climate change [1, 35, 23], with the United States aiming for net-zero emission electricity by 2035 [10]. In alignment with these objectives, Texas, endowed with vast renewable energy resources, has committed to significantly expand its wind and solar power capacities [12, 19, 2]. However, the intermittent nature of these renewable energy sources presents significant challenges to grid stability and reliability, compounded by the uncertainty of the actual total installed capacity in the future and the uncertainty of the growth of future demand for electricity. Without effective solutions, these challenges could lead to potential power outages and inefficiencies in energy supply, undermining the state's renewable energy goals. To address these difficulties, Texas needs to implement additional measures, such as advanced energy storage solutions and grid management technologies [19, 20, 29]. Specifically, integrating hydrogen production and utilization can play a crucial role in stabilizing the grid and enabling more renewable energy generation. This approach not only addresses the current limitations of renewable energy integration but also positions Texas as a leader in the emerging hydrogen economy, with potential economic and environmental benefits (Fig. 1).

Robust energy storage solutions are critical for large-scale renewable deployment, and hydrogen offers a promising option due to its capacity for long-term storage and versatility. Furthermore, Texas has a large-scale industrial demand for hydrogen, particularly in the Gulf of Mexico, where it is used in refining, ammonia production, and chemical processes [3, 27]. Currently, the hydrogen economy is in its nascent stage, with hydrogen production primarily used in industrial applications and accounting for less than 1% of the global energy mix [36]. Scaling hydrogen to support

*Corresponding author.
jiezhang@utdallas.edu (J. Zhang)
ORCID(s): 0000-0002-8405-3032 (H. Li); 0000-0001-7478-5670 (J. Zhang)

Nomenclature

Sets and Collections

I	Set of regions i
K	Set of technologies k
S	Set of scenarios s
T	Set of time periods t

Parameters (Constants)

β	Battery capacity [MWh]
χ	Hourly electricity demand [MWh]
δ	Discount rate [-]
ϵ^{r}	Hourly generation [MWh]
η^{cha}	Charging efficiency [-]
η^{dis}	Discharging efficiency [-]
κ	Hourly hydrogen demand [tons]
λ^{e2h}	Efficiency from electricity to hydrogen [-]
λ^{h2e}	Efficiency from hydrogen to electricity [-]
ρ^{h}	Hydrogen price [k$]
ρ^{o}	Oxygen price [k$]
lifetime	Lifetime of technologies [years]
c^{w}	Water cost per ton [k$]
c^{ins}	Installation cost per technology at each node [k$]
c^{om}	Fixed O&M cost per technology per year [k$]
c^{pen}	Penalty cost per MWh [k$]
c^{p}	CCS cost per ton [k$]
c^{s}	SMR carbon cost per ton [k$]
c^{tr}	Transportation cost per unit [k$]
f^{power}	Gas power emission factor [ton/MWh]
f^{smr}	SMR emission factor [ton/ton]
h^{cost}	Hydrogen price of SMR [k$]
hd_i	Zonal hydrogen demand [tons]
r^{o}	Oxygen rate [tons]
r^{w}	Water rate [tons]

Decision Variables

$\epsilon^{\mathrm{cha}}_{i,t,s}$	Charging in region i, time t, scenario s [MWh]
$\epsilon^{\mathrm{dis}}_{i,t,s}$	Discharging in region i, time t, scenario s [MWh]
$\epsilon^{\mathrm{e2h}}_{i,t,s}$	Electricity to hydrogen in region i, time t, scenario s [MWh]
$\epsilon^{\mathrm{h}}_{i,t,s}$	Electricity from hydrogen in region i, time t, scenario s [MWh]
$\epsilon^{\mathrm{n}}_{i,t,s}$	Electricity purchase in region i, time t, scenario s [MWh]
ψ_i	Hydrogen demand satisfaction rate in region i [-]
$\theta^{\mathrm{b}}_{i,t,s}$	Battery state of charge in region i, time t, scenario s [MWh]
$\theta^{\mathrm{h}}_{i,t,s}$	Hydrogen tank state of charge in region i, time t, scenario s [tons]
$h^{\mathrm{se}}_{i,t,s}$	Hydrogen sold in region i, time t, scenario s [tons]
$h^{\mathrm{smr}}_{i,t,s}$	Hydrogen generated by SMR in region i, time t, scenario s [tons]
$h^{\mathrm{tr}}_{i,j,t,s}$	Hydrogen transfer from region i to j at time t, scenario s [tons]
$o_{i,t,s}$	Oxygen usage in region i, time t, scenario s [tons]
$w_{i,t,s}$	Water usage in region i, time t, scenario s [tons]
$x_{i,k}$	Technology installation in region i and technology k [MW]

renewable energy development requires substantial investment and technological advancements. Challenges include the high cost and limited capacity of electrolyzers, the need for extensive Carbon Capture, Utilization, and Storage (CCUS) for steam methane reforming (SMR) processes, and policy and market acceptance hurdles.

To address these uncertainties and challenges, this study introduces a stochastic optimization model that considers different scenarios of future renewable energy deployment completions and electricity demand growth. Past studies have often focused on changes in renewable energy generation due to meteorological factors [3, 40, 8, 5] and hydrogen's role in decarbonization through infrastructure development and regional hydrogen hubs [24, 43]. Studies have also examined stochastic optimization to address energy uncertainties [45, 44] and the economic implications of hydrogen deployment [41]. Furthermore, advancements in grid flexibility, CCUS technologies, and global case studies on hydrogen integration highlight the potential for achieving cross-sectoral decarbonization [9, 30]. However, this study takes a more macro view, considering the impact of total installed capacity and the growth rate of total energy demand on the energy supply-demand balance. Additionally, it examines the construction of a hydrogen network across Texas within the context of the regional hydrogen hub to address the uneven geographic distribution of energy supply and demand. By incorporating these scenarios, the model provides a more comprehensive and realistic framework for planning and optimizing hydrogen integration. This innovation enhances the resilience and flexibility of the energy system by accounting for uncertainties in future deployment and demand.

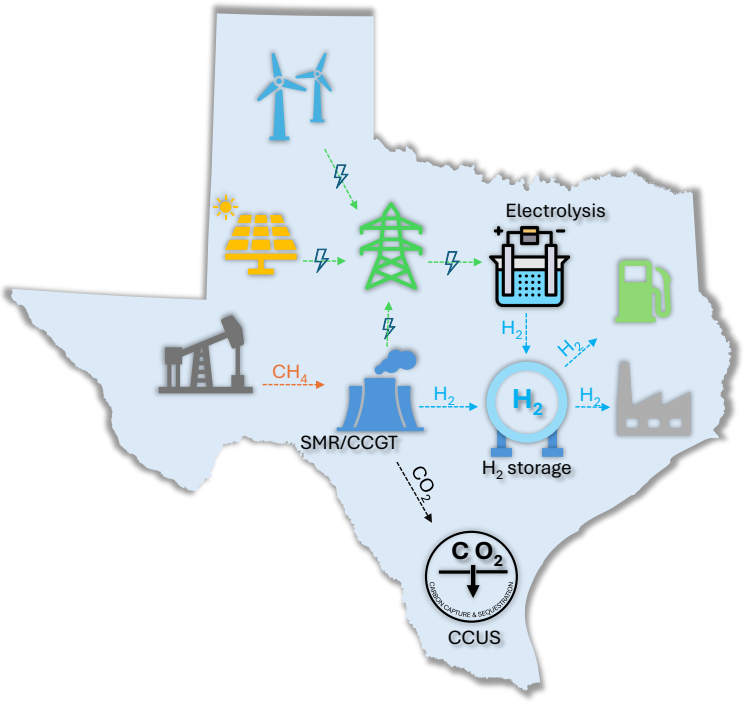


Figure 1: Conceptual Diagram of the Future Texas Power System with Hydrogen Integration. The future Texas power system will rely on combined cycle gas-turbine (CCGT) plants, wind, and solar to meet Electric Reliability Council of Texas (ERCOT)'s demand, with batteries and hydrogen providing energy storage. Natural gas will also produce hydrogen via SMR for industrial use, with CO2 emissions from both gas plants and SMR captured and stored through CCUS technology to achieve zero carbon emissions.

2. Methodology

This study covers the entire ERCOT jurisdiction, dividing it into eight weather zones based on ERCOT's climate zoning. Each zone shares the same meteorological data, meaning generating resources within each zone have the same capacity factor, applicable to both installed and planned resources. The methodology involves a stochastic scenarios design, considering three scenarios for the completion of planned installed capacity: low (0%, status quo, no new equipment installed), medium (30% completion rate), and high (80% completion rate). The probabilities of low, medium, and high scenarios occurring are assumed to be 0.1, 0.7, and 0.2, respectively [38]. For the analysis of electricity demand growth, we added or subtracted 2% from ERCOT's projected 2030 electricity demand for the low and high demand cases, respectively, and projected values for the medium case [17]. The probabilities for the the cases are 0.2, 0.5, and 0.3 (Table 1). By combining these cases, we end up with nine stochastic scenarios and the probability of each occurring is summarized in Table 2. In this study, we focus on addressing the uncertainties associated with future electricity supply and demand. While we acknowledge that future hydrogen demand is also subject to significant uncertainty, obtaining reliable and accurate data on hydrogen demand remains challenging at this time. Additionally, the inherent unpredictability of future hydrogen trends further complicates its modeling. To balance computational complexity with the goal of producing meaningful and referable results, we have assumed a fixed value for future hydrogen demand within the stochastic optimization model.

For the planned additional battery capacity, we assume a 100% completion rate. We also assume that hydrogen demand will remain relatively stable over the next few years, considering factors such as the progress of hydrogen hub completion, penetration of hydrogen vehicles, and changes in hydrogen demand in heavy industry and the petrochemical sector.

The primary data used in the analysis include the existing installed capacities of solar, wind, and battery storage in each region [15], the capacities of various types of equipment scheduled to come online by 2030 [38], and the demand for electricity and hydrogen in each region [12, 16, 3]. This comprehensive approach allows us to accurately model the

Table 1
Uncertainty scenarios for installed capacity and electricity demand growth

Parameters	Scenarios	Decription	Probability
Power demand	Low	2% decrease in ERCOT projections for 2030	0.2
	Medium	ERCOT projections for 2030	0.5
	High	2% increase in ERCOT projections for 2030	0.3
Completion rate of planned installed capacity	Low	0	0.1
	Medium	30%	0.7
	High	80%	0.2

Table 2
Probability of stochastic scenarios

Scenarios	Power demand[a]	Power generation	Probability
1	L	L	0.02
2	L	M	0.14
3	L	H	0.04
4	M	L	0.05
5	M	M	0.35
6	M	H	0.1
7	H	L	0.03
8	H	M	0.21
9	H	H	0.06

[a] L for low case, M for medium case, H for high case.

Table 3
Key parameters used in the stochastic optimization model for the benchmark case study [3, 40, 6, 4, 27].

Category	Items	Value	Unit
General	Electricity to hydrogen (λ^{e2h})	55	kWh/kg
	Hydrogen to electricity (λ^{h2e})	17	kWh/kg
	Battery efficciency ($\eta^{cha//dis}$)	0.95	-
	Hydrogen price (ρ^{h})	4	\$/kg
	Project discount rate (δ)	5%	-
	Life time	30	Year
	Oxygen selling price (ρ^{o})	0.007	\$/kg
	Carbon capture and storage cost (c^{p})	500	\$/T
	Deionized water cost (c^{w})	0.4	\$/kg
	Emission factor (SMR) (f^{smr})	10	T/T
	Emission factor (Power) (f^{power})	0.45	T/MWh
Electrolyzer	Capex cost (c_1^{ins})	588	\$/kW
	O&M cost (c_1^{om})	3.50%	-
	water rate (r^{w})	14.48	\$/kW-year
H_2 Storage	Capex cost (c_2^{ins})	1.296	\$/(km·kW)
	O&M cost (c_2^{om})	5%	-
	Transportation cost per unit (c^{tr})	3	\$/km·T^{-1}
Fuel cell	Capex cost (c_3^{ins})	994	\$/kW
	Fixed O&M (c_3^{om})	13.43	\$/kW-year

impacts of different scenarios on the energy system, providing valuable insights into the future integration of renewable energy and hydrogen in Texas. Some of the key data used in the stochastic optimization model are summarized in Table 3.

The optimization model

This stochastic optimization model aims to optimize the design and operation of a renewable energy system integrated with hydrogen storage and power generation technologies under various stochastic scenarios. The model captures the interplay between energy demand, hydrogen generation, and storage technologies under uncertain future scenarios [28, 26]. The core objective is to minimize the overall costs associated with the energy system, subject to constraints related to energy balance, hydrogen and battery storage, and resource availability.

The objective of the optimization model is to minimize the total system cost, $\mathbb{E}_s(\text{ATC})$, which comprises capital expenditures (Capex) for installing technologies like electrolyzers, fuel cells, and hydrogen storage tanks across regions. These costs are discounted over the lifetime of the technologies using a discount rate, accounting for the time value of money. Additionally, the total cost includes fixed and operational expenditures, $\mathbb{E}_s(\text{O\&M}_s)$, which cover hydrogen transportation, water and oxygen costs, hydrogen production, carbon costs, and penalties for emissions and unmet demand, while also factoring in revenue from the sale of hydrogen and oxygen. The operational expenses, occurring during the runtime phase, are based on expected values across all stochastic scenarios, ensuring that uncertainties in system performance and costs are captured (Eqs. 10, 2, and 3).

Objective function

$$\min \ \mathbb{E}_s(\text{ATC}) = \text{Capex} + \mathbb{E}_s(\text{O\&M}_s) \tag{1}$$

Here, ATC stands for the average total cost (sum of the capital expenditure and the expected operating & maintenance costs). The operator $\mathbb{E}_s(\cdot)$ represents the scenario-weighted expectation over all scenarios s. Capex is the total capital cost, while $\text{O\&M}_s$ denotes the operating & maintenance costs under scenario s.

$$\text{Capex} = \sum_{i=1}^{I} \sum_{k=1}^{K} x_{i,k} \cdot \frac{c_k^{\text{ins}}}{\sum_{\tau=1}^{\text{lifetime}} \frac{1}{(1+\delta)^\tau}} \tag{2}$$

In this expression, $x_{i,k}$ is the installed capacity of technology k in region i, where $k = 1$, 2, and 3 represent the electrolyzer, hydrogen storage tank, and hydrogen fuel cell, respectively. c_k^{ins} is the installation cost per technology, while δ is the discount rate. The denominator $\sum_{\tau=1}^{\text{lifetime}} \frac{1}{(1+\delta)^\tau}$ is the present-worth factor over the lifetime of the technology.

$$\begin{aligned}
\mathbb{E}_s(\text{O\&M}_s) = & \sum_{i \in I} \sum_{k \in K} x_{i,k} \cdot c_k^{\text{om}} \\
& + \sum_{s \in S} \xi_s \left(\sum_{i \in I} \sum_{j \in I} \sum_{t \in T} c^{\text{tr}} \cdot h_{i,j,t,s}^{\text{tr}} \cdot d_{i,j} \right) \\
& + \sum_{i \in I} \sum_{t \in T} c^{\text{w}} \cdot w_{i,t,s} \\
& + \sum_{i \in I} \sum_{t \in T} (c^{\text{s}} \cdot f^{\text{smr}} + h^{\text{cost}}) \cdot h_{i,t,s}^{\text{smr}} \\
& + \sum_{i \in I} \sum_{t \in T} (c^{\text{p}} \cdot f^{\text{power}} + c^{\text{pen}}) \cdot \epsilon_{i,t,s}^{\text{n}} \\
& - \sum_{i \in I} \sum_{t \in T} \rho^{\text{h}} \cdot h_{i,t,s}^{\text{se}} - \sum_{i \in I} \sum_{t \in T} \rho^{\text{o}} \cdot o_{i,t,s}
\end{aligned} \tag{3}$$

Here, c_k^{om} is the fixed O&M cost per technology per year, and ξ_s is the probability of scenario s. c^{tr} is the hydrogen transportation cost per unit, $h_{i,j,t,s}^{\text{tr}}$ is the hydrogen flow from region i to region j at time t and scenario s, and $d_{i,j}$ is the distance between regions i and j. c^{w} is the water cost; $w_{i,t,s}$ is the water usage in region i; c^{s} is the SMR carbon cost; f^{smr} is the SMR emission factor; h^{cost} is the hydrogen price of SMR; c^{p} is the CCS cost; f^{power} is the gas power emission factor; c^{pen} is the penalty cost per MWh; $\epsilon_{i,t,s}^{\text{n}}$ is the purchased electricity; $\rho^{\text{h}}, \rho^{\text{o}}$ are the prices of hydrogen and oxygen, respectively; $h_{i,t,s}^{\text{se}}$ is the hydrogen sold; and $o_{i,t,s}$ is the oxygen usage.

Constraints

The constraints ensure feasible system operation, respecting physical limits and balancing energy/resources. They are grouped for clarity: energy balance, hydrogen balance, storage limits, resource usage, and demand constraints.

$$\epsilon^{\mathrm{h}}_{i,t,s} + \epsilon^{\mathrm{dis}}_{i,t,s} + \epsilon^{\mathrm{n}}_{i,t,s} - \epsilon^{\mathrm{cha}}_{i,t,s} - \epsilon^{\mathrm{e2h}}_{i,t,s} = \chi_{i,t,s} - \epsilon^{\mathrm{r}}_{i,t,s}, \quad \forall i, t, s \tag{4}$$

Equation (4) states the energy balance, where $\epsilon^{\mathrm{h}}_{i,t,s}$ is electricity generated from hydrogen, $\epsilon^{\mathrm{dis}}_{i,t,s}$ is battery discharging, $\epsilon^{\mathrm{n}}_{i,t,s}$ is purchased electricity, $\epsilon^{\mathrm{cha}}_{i,t,s}$ is battery charging, $\epsilon^{\mathrm{e2h}}_{i,t,s}$ is electricity used for hydrogen production, $\chi_{i,t,s}$ is the electricity demand, and $\epsilon^{\mathrm{r}}_{i,t,s}$ is the renewable generation.

$$\theta^{\mathrm{h}}_{i,t,s} = \theta^{\mathrm{h}}_{i,t-1,s} + \sum_{j \neq i} \left(h^{\mathrm{tr}}_{j,i,t,s} - h^{\mathrm{tr}}_{i,j,t,s} \right) + \frac{\epsilon^{\mathrm{e2h}}_{i,t,s}}{\lambda^{\mathrm{e2h}}} - h^{\mathrm{se}}_{i,t,s} - \frac{\epsilon^{\mathrm{h}}_{i,t,s}}{\lambda^{\mathrm{h2e}}}, \quad \forall i, t, s \tag{5}$$

Equation (5) captures hydrogen balance. $\theta^{\mathrm{h}}_{i,t,s}$ is the hydrogen tank's state of charge, λ^{e2h} is the efficiency of electricity-to-hydrogen conversion, and λ^{h2e} is the hydrogen-to-electricity efficiency.

$$\theta^{\mathrm{b}}_{i,t,s} = \theta^{\mathrm{b}}_{i,t-1,s} + \eta^{\mathrm{cha}} \cdot \epsilon^{\mathrm{cha}}_{i,t,s} - \frac{\epsilon^{\mathrm{dis}}_{i,t,s}}{\eta^{\mathrm{dis}}}, \quad \forall i, t, s \tag{6}$$

Equation (6) is the battery storage balance. $\theta^{\mathrm{b}}_{i,t,s}$ is the battery state of charge, η^{cha} and η^{dis} are charging and discharging efficiencies, respectively.

$$\theta^{\mathrm{h}}_{i,t,s} \leq x_{i,2}, \quad \forall i, t, s \tag{7}$$

$$\theta^{\mathrm{b}}_{i,t,s} \leq \beta_i, \quad \forall i, t, s \tag{8}$$

Equations (7) and (8) impose capacity limits on hydrogen tanks $x_{i,2}$ and battery storage β_i, respectively.

$$w_{i,t,s} = r^{\mathrm{w}} \cdot \frac{\epsilon^{\mathrm{e2h}}_{i,t,s}}{\lambda^{\mathrm{e2h}}}, \quad \forall i, t, s \tag{9}$$

$$o_{i,t,s} = r^{\mathrm{o}} \cdot \frac{\epsilon^{\mathrm{e2h}}_{i,t,s}}{\lambda^{\mathrm{e2h}}}, \quad \forall i, t, s \tag{10}$$

Equations (9) and (10) specify water and oxygen consumption for hydrogen production, where r^{w} and r^{o} are the water and oxygen rates per unit of hydrogen produced, respectively.

$$\sum_{s \in S} \xi_s \sum_{t \in T} h^{\mathrm{se}}_{i,t,s} = \psi_i \cdot hd_i, \quad \forall i \in I \tag{11}$$

$$\sum_{s \in S} \xi_s \left(h^{\mathrm{se}}_{i,t,s} + h^{\mathrm{smr}}_{i,t,s} \right) \geq \kappa_{i,t}, \quad \forall i, t \tag{12}$$

Equations (11) and (12) enforce hydrogen demand satisfaction. $h^{\mathrm{se}}_{i,t,s}$ is hydrogen sold, $h^{\mathrm{smr}}_{i,t,s}$ is hydrogen from SMR, ψ_i is the demand satisfaction rate, hd_i is the total hydrogen demand, and $\kappa_{i,t}$ is the hourly hydrogen demand.

$$\epsilon^{\mathrm{h}}_{i,t,s} \leq x_{i,3}, \quad \forall i, t, s \tag{13}$$

$$\epsilon^{\mathrm{e2h}}_{i,t,s} \leq x_{i,1}, \quad \forall i,t,s \tag{14}$$

Equations (13) and (14) limit electricity generation from hydrogen and electricity-to-hydrogen conversion by the installed capacities $x_{i,3}$ and $x_{i,1}$, respectively.

$$\theta^{\mathrm{b}}_{i,0,s} = 0.8 \cdot \beta_i, \quad \forall i,s \tag{15}$$

$$\theta^{\mathrm{b}}_{i,0,s} = 0, \quad \forall i,s \tag{16}$$

Equations (15) and (16) set initial conditions for battery and hydrogen storage, respectively.

$$\epsilon^{\mathrm{n}}_{i,t,s} \leq \max\left(\chi_{i,t,s} - \epsilon^{\mathrm{r}}_{i,t,s}, 0\right), \quad \forall i,t,s \tag{17}$$

Equation (17) restricts hourly power purchase $\epsilon^{\mathrm{n}}_{i,t,s}$ by ensuring it does not exceed the gap between the demand $\chi_{i,t,s}$ and renewable generation $\epsilon^{\mathrm{r}}_{i,t,s}$. This promotes maximum use of renewables while allowing necessary flexibility via CCGT power.

3. Results

3.1. Optimization of the power system

We optimize the energy mix for each zone within the ERCOT [18] by minimizing the total system cost of hydrogen-assisted storage for renewable energy, considering future total installed renewable energy capacity and the capacity of backup combined cycle gas-turbine (CCGT) plants under the uncertainties of both total expected installed capacity of renewable energy and electricity demand growth. The objective is to achieve an optimal balance between renewable and non-renewable energy sources throughout the year. The total system cost includes the capital and operational costs of hydrogen-related equipment, such as electrolyzers, hydrogen storage tanks, and hydrogen fuel cells, as well as the costs associated with hydrogen transportation, and the capture and storage of CO2 produced by SMR processes used for hydrogen production and CCGT for power generation. For electricity from CCGT, we focus solely on the wholesale tariffs and the costs of CO2 mitigation from these plants, rather than the expenses of constructing new gas-fired power plants. This approach ensures a comprehensive assessment of the economic implications of integrating hydrogen storage into the renewable energy framework, providing a clear understanding of the trade-offs and benefits associated with different energy mix scenarios, and enabling the development of a cost-effective and sustainable energy strategy for Texas (Fig. 2).

Taking into account the planned installed capacity of each region, the possible percentage of completion, the demand for electric energy, the uncertainty in the growth rate of electric energy, the capacity factor of wind and other resources, we prioritized renewable energy [38, 16, 15]. In this study, we assume that renewable energy is first supplied to meet the demand for electric energy, and any surplus is used for hydrogen production. Additionally, we consider the carbon dioxide factor of CCGT, hydrogen demand, and the efficiency of the conversion between hydrogen and electricity. Based on these factors, we determined the optimal values for required installed capacity of CCGT, the green hydrogen (electrolyzers with renewable energy) fulfillment rate, the state of charge of the battery, and the state of the hydrogen tanks in each region, as summarized in Table 4. As shown in Fig. 4**a**, the stochastic optimization effectively balances the system's power supply. During peak renewable energy generation, excess electricity is stored in batteries, while a portion is converted to green hydrogen via electrolyzers. In low generation periods, the system meets demand by drawing on stored energy from both batteries and CCGT, ensuring continuous stability.

It is observed that there are spatial and temporal differences in power generation between regions, such as hourly and seasonal variations (Fig. 3 **a, b**), and differences in geographic location (Fig. 3 **c, d**). These differences are influenced by the climatic variations across regions and the different proportions of solar and wind energy installations. As a result, power generation in these regions is often out of sync with the electricity demand curve. To address this, our model incorporates the scenario of load demand flexibility. By adding an acceptable range (±5% power demand) to the hourly power demand while maintaining the total power demand constant, we shift power demand to align more closely with the characteristics of renewable energy generation. This approach maximizes the use of renewable energy

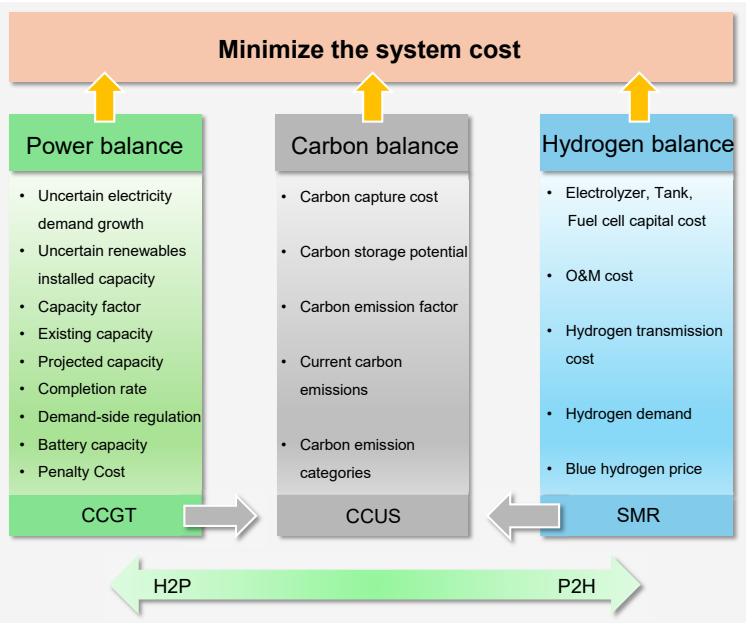


Figure 2: Structural Diagram of the Stochastic Optimization Model. This model focuses on maintaining three key system balances: electricity demand, hydrogen demand, and carbon balance. The carbon balance addresses CCUS from CCGT and SMR processes. Hydrogen and electricity are interconverted via electrolyzers and hydrogen fuel cells to maintain equilibrium between electricity and hydrogen demand. The core influencing factors of these balances are the primary focus of the model, with the objective function aiming to minimize the total cost of maintaining these three critical balances.

Table 4
Results for CCGT capacity, green hydrogen rate, and storage unit status for each region in the benchmark case.

	Coast	East	Far west	North	North center	South	South center	West
CCGT (MW)	22,719	3,116	11,258	26,535	2,488	16,571	7,777	1,865
Green H2 rate	0	87.78%	59.33%	5.20%	NA	0	92.93%	NA
State of charge	55.99%	60.14%	60%	24.47%	69.37%	60.88%	46.62%	73.71%
State of tank	NA	36.11%	NA	NA	34.3%	NA	NA	NA

and minimizes reliance on non-renewable sources. The total annual electrical energy demand for CCGT across the entire ERCOT region experienced a slight decline, dropping from 389,785,123 MWh to 389,164,389 MWh. Similarly, the total annual demand for blue (SMR with CCUS) hydrogen showed a marginal reduction, decreasing from 3,309 kilotons (KT) to 3,307 KT. Fig. 4**b** illustrates the difference between the original power demand and the adjusted power supply curve following load regulation. The visualization clearly shows that demand-side load regulation effectively shifts the demand peaks, aligning them more closely with the system's generation profile. This adjustment improves the balance between generation and consumption, optimizing efficiency and easing the strain on resources during peak demand.

To refine our analysis, we designed several sensitivity experiments to explore the robustness of our model under varying conditions. For scenarios A1 and A2, we varied the completion rate of the planned installed renewable energy capacity by $\pm 10\%$ for both medium and high completion cases. In scenarios A3 and A4, we analyzed the effects of adjusting the growth rate of electricity demand by $\pm 5\%$ for each case. Lastly, for scenarios A5 and A6, we reduced the final installed capacity of the planned energy storage systems to 80% and 60% of the target levels. These sensitivity analyses provide insights into the impact of key variables on overall system performance, helping us identify potential risks and opportunities(Table 5).

The results reveal the impact of completion rates (defined in the Methods section) of planned renewable energy capacities on future energy system operating costs and the operation of other equipment within the system. Higher

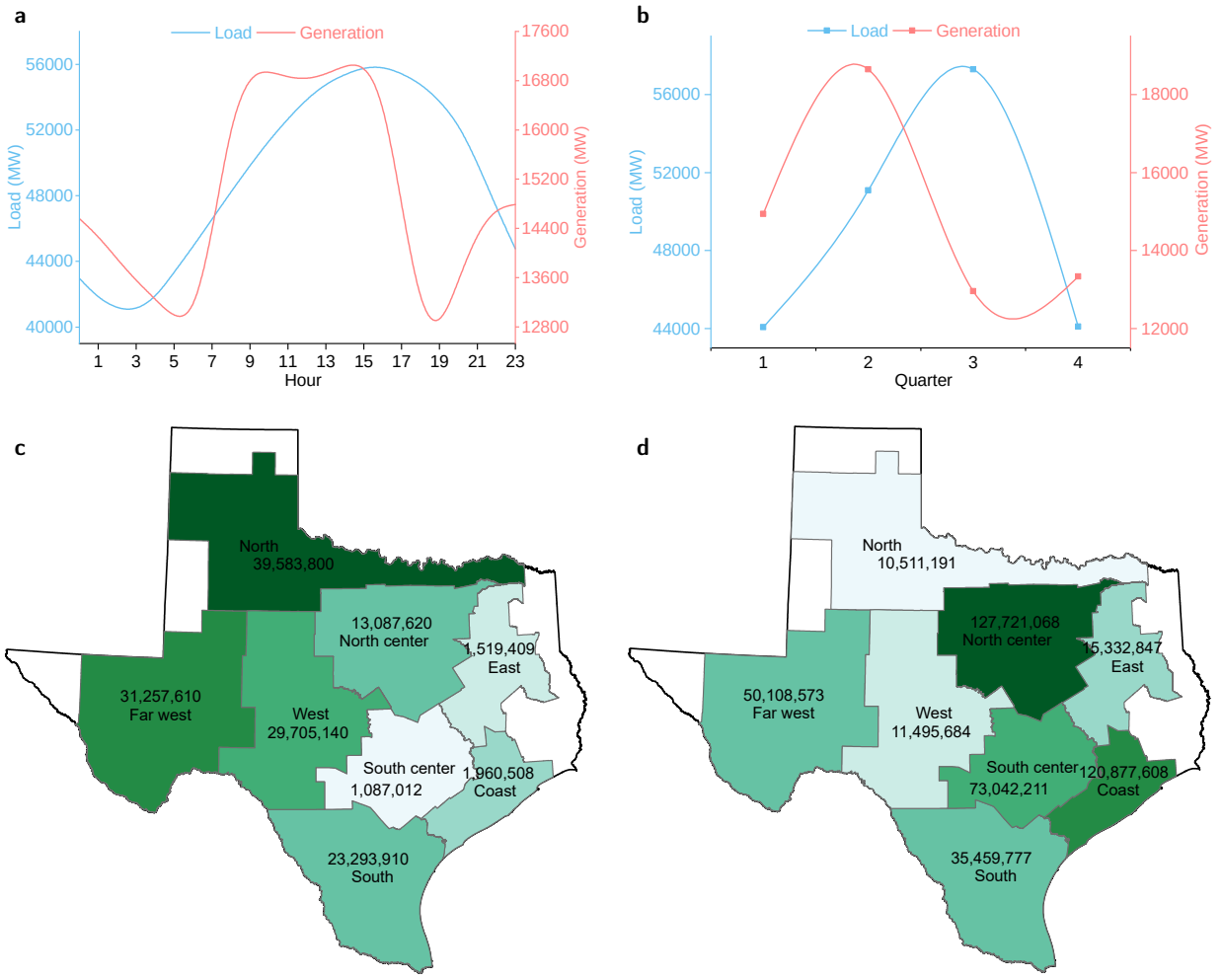


Figure 3: Spatial and Temporal Differences Between Renewable Energy Generation and Electricity Demand in ERCOT. a shows that peak renewable energy generation in ERCOT occurs between 9am and 3pm, while peak electricity consumption is concentrated from 3pm to 7pm. Seasonally, **b** depicts renewable energy generation peaks in the second quarter, whereas electricity demand peaks in the third quarter. These mismatches highlight the need for both short- and long-term storage solutions to enhance renewable energy integration into the ERCOT grid. Figures **c** and **d** illustrate the spatial distribution of renewable energy generation and electricity demand across the eight weather zones within ERCOT (Both are results for 2023, in kW), with darker colors representing higher values. The data reveal a clear spatial disparity: renewable energy generation is primarily concentrated in the Midwest region, while electricity demand is predominantly focused in the Southeast and North regions, highlighting significant geographic differences in supply and demand.

completion rates of planned renewable energy capacities significantly decreased the total system cost by utilizing more low-cost renewable energy sources (i.e., from $150.5 billion to $146.8 billion). Conversely, lower completion rates increased costs (i.e., from $150.5 billion to $154.4 billion), highlighting the economic benefits of higher renewable energy penetration. At the same time, the supply of green hydrogen within ERCOT increases by 10,844 tons (+8%) in the higher completion rate scenario, and decreases by 15,412 tons (-12%) in the lower completion rate scenario. Meanwhile, the circulation of hydrogen increases by 5,979 tons (+5%) and 9,035 tons (-7%) in the higher and lower completion rate scenarios, respectively. In terms of the utilization of energy storage and hydrogen storage equipment, the increased completion rate has simultaneously driven a more efficient use of these storage systems. Notably, battery utilization has reached an average of 64.8%, corresponding to 68,698 MWh of stored energy, up from a previous average of 56.3% or 59,312 MWh. This trend highlights the critical role of energy storage in accommodating the growing penetration of renewable energy sources. As renewable energy continues to expand, the need for higher capacity storage

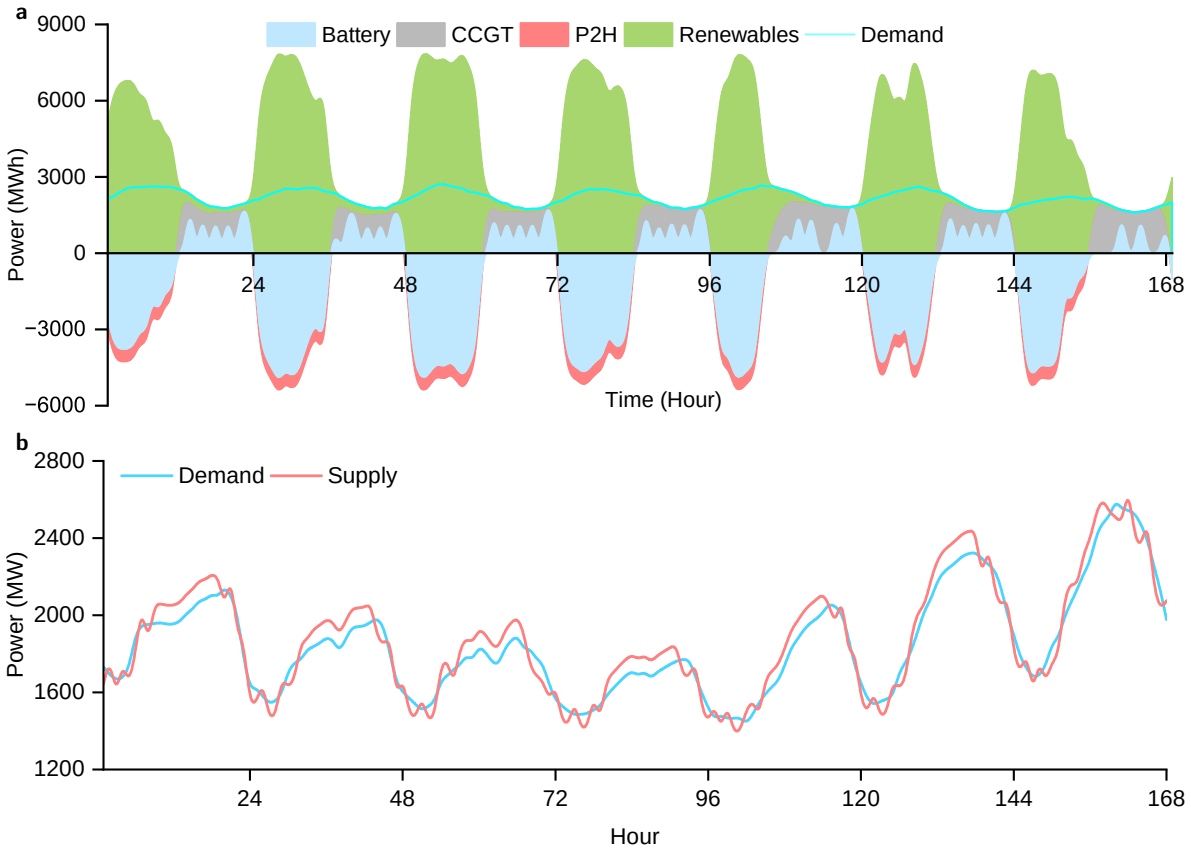


Figure 4: Results of Power System Optimization. a, Stochastic optimization results showing power balance within the system. During peak clean energy generation, excess electricity is stored in batteries, while some is converted into green hydrogen via electrolyzers. In periods of low generation, stored energy from batteries and CCGT work together to meet power demand, maintaining system stability. **b**, The difference between original power demand and actual power supply after load regulation. Demand-side adjustments successfully shift peak demand periods to better align with the system's power generation profile.

Table 5
Sensitivity analysis scenarios for optimization of the power system

Scenarios	Description
A1	+ 10% completion rate of projected renewables installation
A2	- 10% completion rate of projected renewables installation
A3	+ 5% final power demand
A4	- 5% final power demand
A5	80% completion rate of projected battery installation
A6	60% completion rate of projected battery installation

systems becomes increasingly evident to manage and balance the inherent fluctuations in energy supply, ensuring a stable and reliable energy system.

3.2. Analysis and optimization of hydrogen systems

This study investigates the dual role of hydrogen in increasing renewable energy penetration and supporting decarbonization in Texas. Hydrogen acts as an energy storage medium for managing renewable intermittency and as a clean fuel to reduce emissions. We analyzed hydrogen demand across eight weather zones, detailed in Fig. 5. The Gulf Coast, a major hub for U.S. hydrogen demand, driven by ammonia, methanol, and refinery industries, consumes over 3 megatons annually ($MT \cdot yr^{-1}$), over a quarter of the national demand [42, 14]. About half of U.S. hydrogen

production is concentrated in this region, where Air Products operates the world's largest hydrogen pipeline network [37]. The region also hosts a significant portion of the nation's hydrogen pipelines. As of December 2020, the U.S. had over 1,600 miles of hydrogen pipelines, nearly all of which are located in Texas and Louisiana[39]. These factors position the Gulf Coast as a foundation for a cleaner hydrogen market. However, geographical discrepancies between hydrogen demand and renewable generation prompted the design of a green hydrogen transportation network within ERCOT (Fig. 6**a**). Hydrogen is transported between neighboring zones. Electrolyzers, storage tanks, and fuel cells are installed at zone nodes to optimize hydrogen's energy storage potential, with surplus renewable energy converted to hydrogen. While hydrogen demand is met by SMRs, we accounted for carbon capture costs. Electrolyzer capacity was capped at 500 MW, considering spatial constraints.

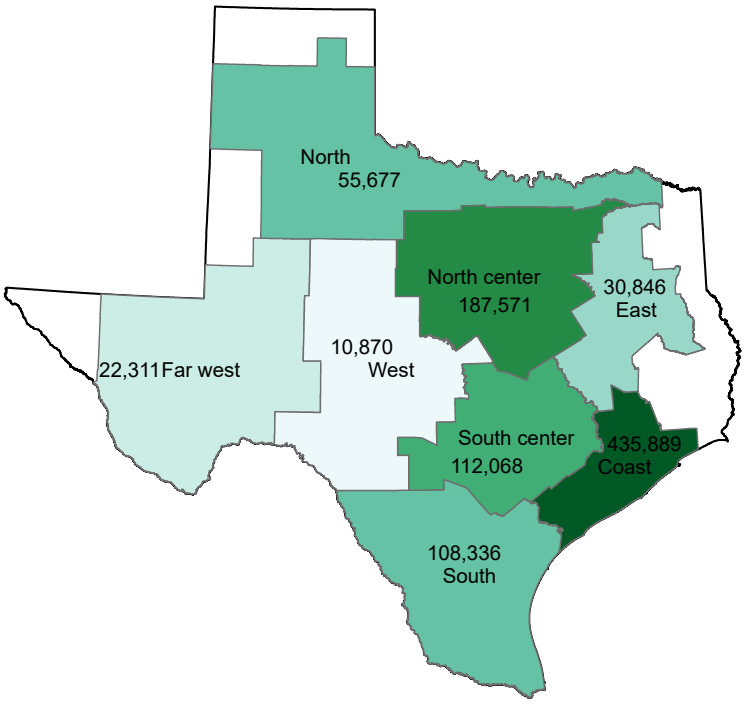


Figure 5: Hydrogen demand (kg/Day)

The results of the stochastic optimization reveal that 3.8% of the hydrogen demand within ERCOT will be met by green hydrogen. The results also revealed an unexpected strategy: instead of installing the electrolyzer in the region with the highest hydrogen demand, the system opted to place the electrolyzer in areas with minimal or even no hydrogen demand. This decision was driven by the economic efficiency of inter-regional hydrogen transportation (Fig. 6a), and the availability of renewable energy (Fig. 3c). This conclusion is supported by the economically optimal results generated by the stochastic optimization model, which aims to minimize total system costs. In Zone East and Zone North Center, 49 tons and 14 tons hydrogen storage tanks were strategically installed to address the mismatch between hydrogen production and demand. Fig. 6**b** illustrates the hydrogen transfer between the eight regions, showing a predominant flow direction from west to east and from north to south. Notably, Zone South Center meets 92.9% of its total hydrogen demand through supply from the two green hydrogen production zones. However, despite Zone Coast and Zone South being the regions with the highest hydrogen demand, the most economical solution to meet their needs, given the current green hydrogen production capacity, is to rely entirely on gray hydrogen. This approach highlights the complex interplay between production capabilities, regional demands, and economic viability within the hydrogen supply network.

A series of sensitivity analyses were conducted to assess the impact of technological advancements on cost reductions. In the first category of scenarios, we examined the effects of reducing the initial costs of hydrogen-related equipment, including electrolyzers, hydrogen storage tanks, and hydrogen fuel cells, by incremental percentages of 5%, 10%, 15%, 30%, and 50%. These scenarios are designed to assess how these cost reductions influence the economic

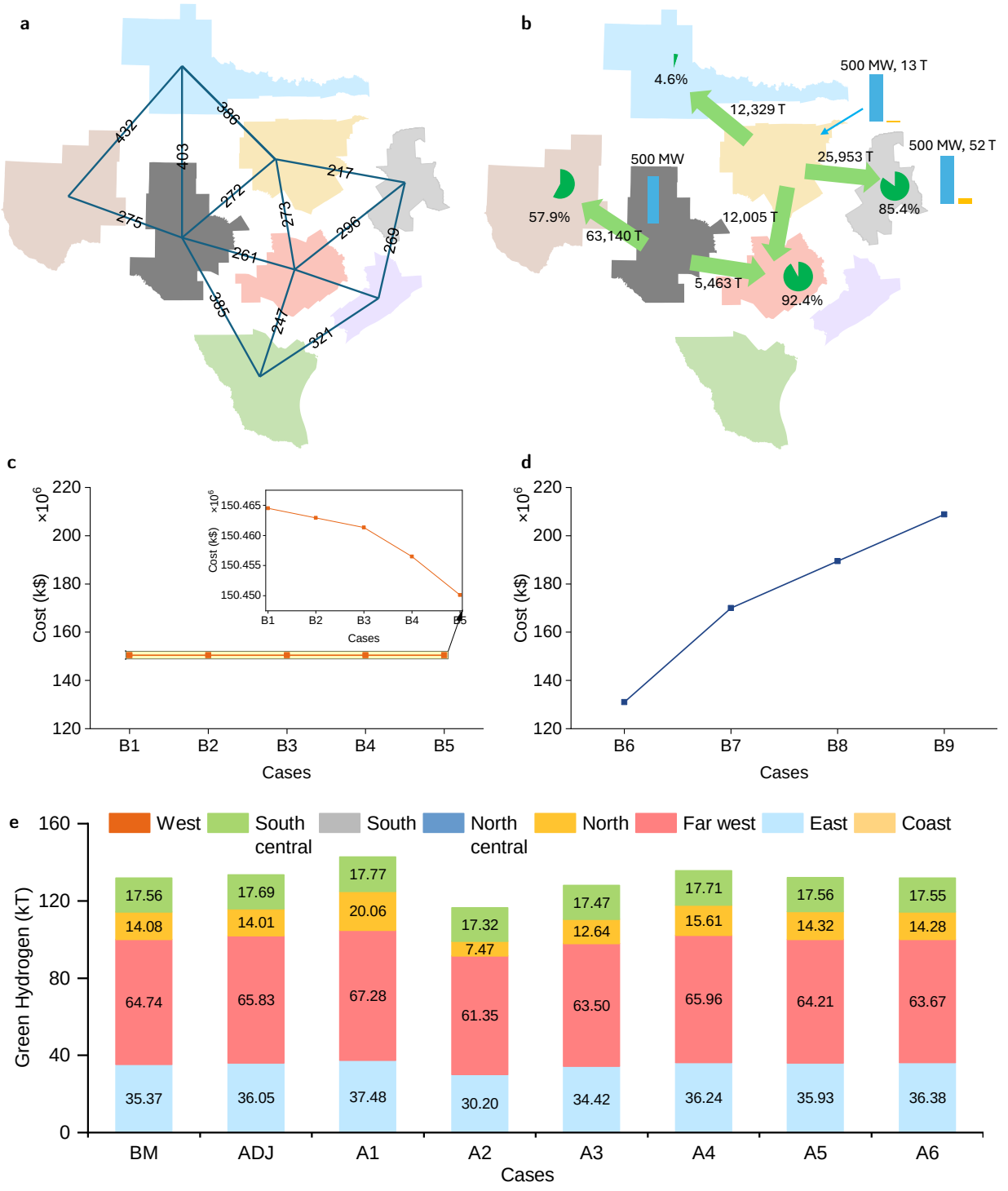


Figure 6: Inter-Zone Hydrogen Network in ERCOT and Results. a, The model assumes that hydrogen pipelines can only connect two adjacent weather zones within ERCOT, with the straight-line distance between zone centers (in kilometers) determining hydrogen transportation costs. **b**, Stochastic optimization results show that the system strategically installs electrolysis units in central zones, using the hydrogen network to transport green hydrogen to surrounding zones, optimizing both production and distribution efficiency. **c** and **d**, Changes in the total cost of cases in the sensitivity analysis. As the initial cost of hydrogen-related equipment decreases, the total system cost decreases, and the increase in CCGT tariffs substantially increases the total system expenditures. **e**, Green hydrogen volume in weather zones in sensitivity analysis in the case of power system optimization.

Table 6
Sensitivity analysis scenarios for analysis and optimization of hydrogen systems

Scenarios	Description
B1	- 5% Capex of hydrogen-related equipment
B2	- 10% Capex of hydrogen-related equipment
B3	- 15% Capex of hydrogen-related equipment
B4	- 15% Capex of hydrogen-related equipment
B5	-50% Capex of hydrogen-related equipment
B6	\$50MWh^{-1} wholesale electricity price
B7	\$150MWh^{-1} wholesale electricity price
B8	\$200MWh^{-1} wholesale electricity price
B9	\$250MWh^{-1} wholesale electricity price

viability and adoption rates of green hydrogen technologies within the energy system. In the second category of scenarios, we modified the electricity tariff of the backup gas-fired power plants to explore how increases in this tariff affect the overall system configuration. This scenario allowed us to observe the shifts in the energy mix and the reallocation of resources within the system as the cost of backup electricity rises. (Table 6).

The results show that reducing the cost of hydrogen equipment alone did not significantly alter the system's configuration, changes in electricity prices from CCGT had a profound effect on the energy mix and deployment strategy. When electricity prices rose to \$200 MWh^{-1}, the total installed capacity of CCGT plants dropped from 92,329 to 92,176 MW, while hydrogen fuel cell capacity increased from 0 to 296 MW. This led to greater use of green hydrogen as an energy reserve, with stored hydrogen being converted to electricity during periods of low renewable generation. Consequently, the total green hydrogen supply fell from 131,748 T to 40,232 T, while hydrogen-to-electricity conversion surged to 1,789,688 MWh. Despite a 50% cost reduction in hydrogen technologies, they still struggle to compete with gas-fired backup electricity. The system's sensitivity to electricity prices highlights its reliance on gas-fired plants, emphasizing the need for further cost reductions and advancements in hydrogen technologies to enhance their competitiveness and influence in the energy mix. It is worth noting that the focus of this study is to optimize the structure of the energy system under the uncertainty of future electricity supply and demand, and the adjustment of electricity prices in the sensitivity analysis is only intended to show the direct impacts it brings to the energy system, but it does not take into account the possible secondary economic effects of the electricity price increase, such as the impacts on household incomes or industrial productivity, which require further in-depth analysis beyond the scope of this study. Table 7 shows the difference in capacity of hydrogen-related equipment in each case of the sensitivity analysis

3.3. CO2 emission abatement analysis

Most of the world's environmental challenges stem from carbon emissions [7]. Global energy-related CO2 emissions surged by 1.1% in 2023, rising by 410 MT to hit an unprecedented record of 37.4 GT [22, 31]. As such, a key goal in energy system development is to reduce carbon emission, and increasing the penetration of renewable energy sources is a crucial part of this effort. However, the volatility of renewable energy necessitates reliable energy storage solutions, and hydrogen emerges as a versatile option. It not only serves as a medium for long-term energy storage but also acts as an industrial feedstock, particularly useful in hard-to-decarbonize sectors, further aiding in the reduction of carbon emissions. This section of the study focuses on this context, using Texas's 2022 carbon emissions data as a reference [13]. As illustrated in Fig. 7, direct combustion and power generation contribute 28% and 54% of Texas's total carbon emissions, respectively, while other sectors account for only 18%. Therefore, targeting carbon reductions in the areas of power generation and direct combustion presents the most impactful strategy for significantly lowering Texas's overall carbon emissions.

At the current stage, the penetration of renewable energy sources remains relatively low (30% [11]), leaving the power system reliant on fossil fuels, either as a backup supply or as a direct part of the energy mix. Consequently, reducing carbon emissions from the energy supply side is critical, but CCUS also plays a pivotal role in emission reduction strategies [33]. Texas is particularly well-positioned to capitalize on its unique geologic structures for CCUS to further minimize its carbon footprint. The state's vast subsurface geology offers numerous potential sites for storing captured carbon dioxide, including depleted oil and gas fields, saline aquifers, and unmineable coal seams [25]. The Gulf Coast region stands out, offering opportunities for both enhanced oil recovery (EOR) and permanent CO2

Table 7
The optimal capacity of hydrogen-related equipment

	B1	B2	B3	B4	B5	B6	B7	B8	B9
East 1[a,b]	500	500	500	500	500	500	500	500	500
East 2	51	47	47	47	53	49	47	47	99
East 3	0	0	0	0	0	0	0	134	178
East 1	0	0	0	0	0	0	0	0	0
Far west 2	0	0	0	0	0	0	0	0	0
Far west 3	0	0	0	0	0	0	0	0	0
North 3	0	0	0	0	0	0	0	0	0
North center 1	500	500	500	500	500	500	500	500	500
North center 2	15	19	19	22	22	15	17	27	3
North center 3	0	0	0	0	0	0	0	2	0
South center 2	0	0	0	0	0	0	0	0	14
South center 3	0	0	0	0	0	0	0	153	271
West 1	500	500	500	500	500	500	500	500	500
West 2	0	0	0	0	0	0	0	0	19

[a] The first two digits are the weather zone code, the last digit is the technology, 1 is the electrolyzer, 2 is the hydrogen tank, and 3 is the fuel cell.
[b] Electrolyzers are measured in MW, hydrogen tank in T, and fuel cells in MW.

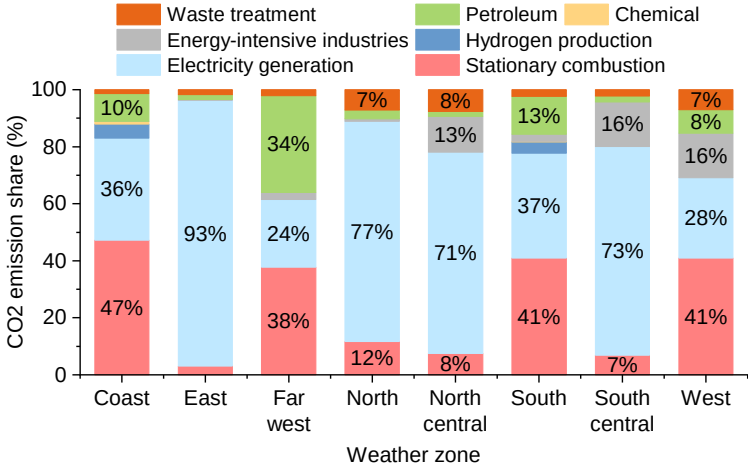


Figure 7: CO2 Emission Percentage. The figure illustrates the carbon emission shares from various energy sources across ERCOT's zones: Coast, East, Far West, North, North Central, South, South Central, and West. Direct combustion and electricity generation account for over 60% of total carbon emissions in each region. In Zone East, electricity generation contributes a staggering 93.3% of the region's emissions due to its low renewable energy penetration and distance from major wind and solar hubs in the Midwest. Zone Far West, a key fossil fuel production area, sees 33.9% of its emissions coming from oil-related activities. Meanwhile, Zone Coast, despite being a core petrochemical region, has minimal petroleum-related emissions, primarily because hydrogen used in its production processes is supplied from other Gulf Coast states, reducing reliance on local fossil fuels. These patterns underscore the regional differences in carbon emissions, driven by geographic, industrial, and energy resource factors across ERCOT's territory.

storage within its expansive saline aquifers and depleted oil fields [32]. According to the National Energy Technology Laboratory (NETL), Texas's saline formations alone could store up to 20 billion metric tons of CO2 [21, 34]. Integrating CCUS with renewable energy and hydrogen solutions creates a comprehensive approach to achieving substantial carbon reductions. In this study, we focus on the cost implications of implementing CCUS in CCGT and SMR units, examining how these factors affect the overall system cost, energy mix, and future composition of the energy system.

Table 8
Optimal sizes of hydrogen related equipment for C4

	Coast	East	Far west	North	North center	South	South center	West
Electrolyzer (MW)	0	500	500	0	500	0	0	500
Tank (T)	0	117	33	0	28	0	9.8	18
Fuel cell (MW)	0	219	22	105	2.5	0	237	0

The results of our stochastic optimization reveal that by 2030, if ERCOT's electricity demand is met solely by a combination of wind, solar, and CCGT, the expected CO2 emissions from CCGT, considering various stochastic scenarios, would reach 175.4 MT per year. However, by implementing load regulation on the demand side, these emissions are reduced by 279 KT (Fig. 8**a**). Additionally, our analysis shows that in scenarios where the electricity price from CCGT remains below $200 per MWh, the structure and composition of the energy system remain unchanged, resulting in no reduction in overall carbon emissions. In contrast, when the price increases to $200 and $250 per MWh, the system compensates by installing more hydrogen fuel cells to meet electricity demand, reducing CO2 emissions from CCGT to 174.6 MT and 174.4 MT, respectively. However, this shift necessitates greater reliance on gray hydrogen to meet hydrogen demand, which subsequently raises CO2 emissions (Fig. 8**b**). Furthermore, the inefficiency in converting electricity to hydrogen and then back to electricity results in energy losses, leading to an overall increase in total system CO2 emissions. In sensitivity analyses that adjust the cost of hydrogen-related equipment (Table 6), we observe no significant change to the energy system configuration, and thus the total carbon emissions remain unchanged. This underscores the complexity of balancing cost, emissions, and system efficiency in future energy scenarios. The carbon emissions reduction results presented in this study should be interpreted as an indicator of the effectiveness of the stochastic optimization approach rather than its ultimate goal. The relatively modest reduction of 1,300 tons of CO2 reflects the structural challenges within ERCOT's energy system, where limited renewable energy penetration and a reliance on fossil fuels drive high baseline emissions. While the optimization framework minimizes system costs rather than maximizing emissions reductions, these results provide valuable insights into the interplay between carbon mitigation and system economics, offering a foundation for further exploration of clean energy deployment strategies.

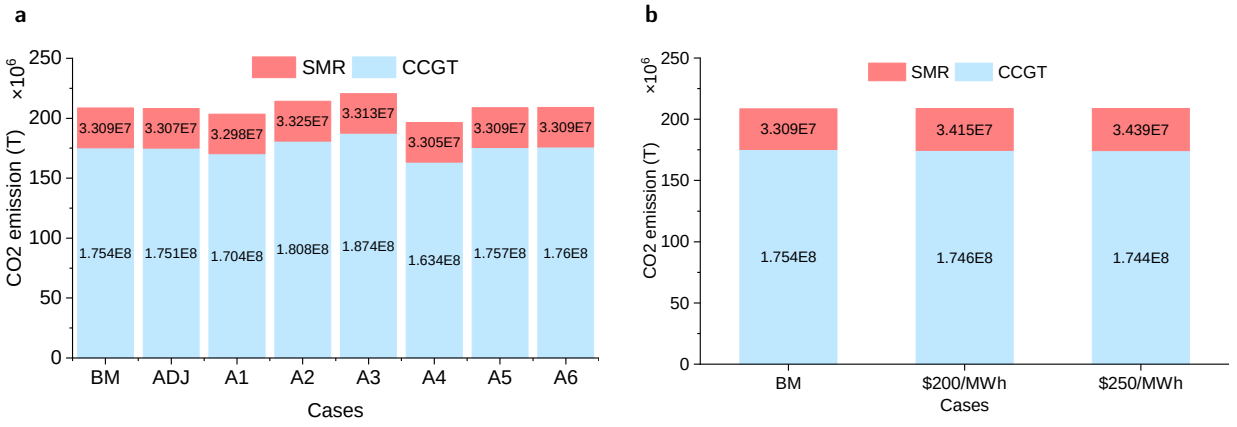


Figure 8: Results of Sensitivity Analysis on Carbon Emissions. a, Through demand-side load regulation, renewable energy utilization becomes significantly more efficient, leading to notable reductions in carbon emissions from both SMR and CCGT. Completion rates and electricity demand directly impact these emissions, with low completion rates and high demand increasing emissions from both sources. Reduced battery installation completion lowers renewable energy flexibility, decreasing utilization rates and raising CCGT emissions, while SMR emissions remain unaffected. **b**, Higher CCGT tariffs lead to increased conversion of green hydrogen to electricity, lowering overall electricity use efficiency. This shift raises carbon emissions from SMR and the overall system, despite a reduction in emissions from CCGT.

To better understand the impact of CCUS costs on the overall system performance, we conducted a sensitivity analysis by varying carbon pricing. In Scenarios 1 and 2, the cost of CCUS was increased to $100 and $150 per ton

Table 9
Sensitivity analysis scenarios for CO2 emission abatement analysis

Scenarios	Description
C1	\$100 Carbon capture and storage costs
C2	\$150 Carbon capture and storage costs
C3	\$50 Power, \$150 SMR
C4	\$150 Power, \$50 SMR

across the entire system, respectively. In Scenarios 3 and 4, we raised the CCUS cost to \$150 per ton for either SMR or CCGT individually, while maintaining the cost at \$5 per ton for the other, to assess the impact on system configuration (Table 9).

In the first three scenarios, the higher CCUS cost for SMR prompted the system to install a 500 MW electrolyzer in the Far West region, reducing overall reliance on gray hydrogen and thus lowering total carbon emissions. However, in Scenario C4, where only the CCUS cost for CCGT was increased (assumed the CCUS cost is higher than that for SMR), total carbon emissions rose. This was primarily due to the increased cost of CCUS for CCGT, making the system less efficient in managing emissions. Additionally, as shown in Table 8, a large number of hydrogen fuel cells were installed (586 MW), leading to more green hydrogen being converted to electricity to meet system demand. This shift forced the system to rely more heavily on gray hydrogen to satisfy hydrogen demand. As previously discussed, the inefficiency of the hydrogen-to-electricity cycle resulted in significant energy losses, further contributing to an overall increase in carbon emissions. This highlights the trade-offs between system configuration, energy efficiency, and emission outcomes as CCUS costs fluctuate.

4. Conclusion and Discussion

This study underscores hydrogen's pivotal role in enhancing renewable energy integration and driving decarbonization within Texas's energy system. Through comprehensive modeling and analysis, we demonstrate that hydrogen, when integrated with renewable sources such as wind and solar, serves not only as a crucial energy storage medium but also as a versatile fuel that can address the intermittency of renewable generation. By strategically placing electrolyzers in high-renewable, low-demand regions, hydrogen can contribute significantly to grid stability and flexibility. Moreover, the development of a hydrogen transportation network enables efficient energy distribution across regions, meeting up to 92.4% of hydrogen demand in certain areas and reducing the need for fossil fuel-based generation.

Despite these promising results, several limitations must be acknowledged. The scenarios modeled, while extensive, contain inherent uncertainties, particularly related to the completion rates of planned renewable installations and the actual behavior of the market in future decades. These uncertainties, while managed through careful assumption-setting, suggest that our findings should be interpreted as directional insights rather than precise forecasts. At the same time, this study does not explicitly model future changes in renewable energy costs, such as increased land costs due to siting challenges or cost reductions from technological advancements. Instead, these factors are indirectly reflected in the planned installed capacity completion rate, assuming that cost dynamics will influence project implementation in a market-driven economy. This study specifically focuses on hydrogen transportation via pipelines, given its relevance to large-scale and long-term deployment within the Texas energy system. Other potential transportation methods, such as road transport (e.g., tube trailers) and rail, were not included in the current model to maintain a clear focus on the primary objective of addressing electricity supply-demand uncertainty and optimizing the role of hydrogen in this context. However, we acknowledge that these alternative transport methods could significantly influence the economic and operational performance of the system. Future research will aim to incorporate these modes of transportation, along with additional storage options such as salt caverns, to develop a more comprehensive and integrated hydrogen energy system model. Furthermore, while we accounted for the costs of CCUS in our carbon emissions analysis, we did not fully address the installation and capacity constraints of CCUS infrastructure. This represents another area for future investigation to ensure the feasibility of large-scale CCUS deployment. Given the focus and scope of this study, we have conducted our analysis of carbon emission reduction results at the level of the entire ERCOT system, rather than delving into the detailed emissions across the full lifecycle of the system. While this approach aligns with the primary objectives of our research, we recognize the importance of a more granular and comprehensive evaluation.

In future studies, particularly when examining the environmental and social value of hydrogen, we plan to conduct a more thorough and detailed analysis of carbon emission reductions, encompassing lifecycle considerations to provide a holistic perspective. As previously mentioned, this study does not incorporate the uncertainty of future hydrogen demand into the stochastic optimization model. This decision was made after carefully considering the limitations in the accuracy of available hydrogen demand data, the primary focus of this paper, and the challenges posed by computational complexity. However, we recognize the importance of addressing this uncertainty to enhance the comprehensiveness of our analysis. In future studies, we plan to integrate hydrogen demand uncertainty into our models to develop a more unified and holistic energy system framework.

Our sensitivity analyses reveal that reductions in hydrogen equipment costs alone are insufficient to drastically reshape the energy system. However, rising electricity prices from gas-fired plants do have a substantial impact on the system's configuration, emphasizing the need for policy-driven investments in hydrogen infrastructure and technological advancements. Policy support will be critical in fostering the growth of hydrogen and renewable energy, particularly in building regional hydrogen hubs and advancing CCUS technologies. These elements are essential for aligning Texas's energy system with its long-term decarbonization goals and national climate objectives.

In conclusion, hydrogen is positioned as a vital component in Texas's future energy landscape. Its dual role as an energy storage medium and a clean fuel allows it to effectively balance the variability of renewable generation, while its versatility extends to decarbonizing hard-to-electrify sectors such as heavy industry and transportation. Although uncertainties remain regarding the completion of renewable energy projects and the deployment of hydrogen infrastructure, the potential benefits of hydrogen integration are clear. With continued policy support, investments in hydrogen infrastructure, and advancements in CCUS technologies, Texas has the opportunity to achieve a more resilient, flexible, and low-carbon energy system. Hydrogen stands as a key enabler of this transition, helping the state meet its renewable energy and carbon reduction targets, ensuring a sustainable energy future.

Declaration of competing interest

The authors declare that they have no known competing financial interests or personal relationships that could have appeared to influence the work reported in this paper.

Acknowledgments

This work was supported by the National Science Foundation under grant 2229417 and the Hydrogen INTERN program.

References

[1] P. Agreement. Paris agreement. In report of the conference of the parties to the United Nations framework convention on climate change (21st session, 2015: Paris). Retrived December, volume 4, page 2017. HeinOnline, 2015.

[2] S. Badakhshan, S. Senemmar, H. Li, and J. Zhang. Integrating offshore wind farms with unmanned hydrogen and battery ships. In 2022 IEEE Kansas Power and Energy Conference (KPEC), pages 1–6. IEEE, 2022.

[3] E. F. Bødal, D. Mallapragada, A. Botterud, and M. Korpås. Decarbonization synergies from joint planning of electricity and hydrogen production: A texas case study. International Journal of Hydrogen Energy, 45(58):32899–32915, 2020.

[4] T. Borsboom-Hanson, S. R. Patlolla, O. E. Herrera, and W. Mérida. Point-to-point transportation: the economics of hydrogen export. International Journal of Hydrogen Energy, 47(74):31541–31550, 2022.

[5] A. Choukulkar. Don't Mess with Texas: Getting the Lone Star State to Net-Zero by 2050. University of Colorado Boulder, 2022.

[6] K. de Kleijne, M. A. Huijbregts, F. Knobloch, R. van Zelm, J. P. Hilbers, H. de Coninck, and S. V. Hanssen. Worldwide greenhouse gas emissions of green hydrogen production and transport. Nature Energy, pages 1–14, 2024.

[7] J. Delbeke, A. Runge-Metzger, Y. Slingenberg, and J. Werksman. The paris agreement. In Towards a climate-neutral Europe, pages 24–45. Routledge, 2019.

[8] P. Denholm, D. J. Arent, S. F. Baldwin, D. E. Bilello, G. L. Brinkman, J. M. Cochran, W. J. Cole, B. Frew, V. Gevorgian, J. Heeter, et al. The challenges of achieving a 100% renewable electricity system in the united states. Joule, 5(6):1331–1352, 2021.

[9] P. Denholm and M. Hand. Grid flexibility and storage required to achieve very high penetration of variable renewable electricity. Energy Policy, 39(3):1817–1830, 2011.

[10] DOE. On the path to 100% clean electricity. [Online] Available at: https://www.energy.gov/policy/articles/path-100-clean-electricity. [Accessed: 25 Dec. 2023].

[11] EIA. Hourly generation by energy source. [Online] Available at: https://www.eia.gov/opendata/browser/electricity/rto/fuel-type-data. [Accessed: 25 Aug. 2024].

[12] EIA. Solar capacity additions are changing the shape of daily electricity supply in texas. [Online] Available at: https://www.eia.gov/todayinenergy/detail.php?id=61783. [Accessed: 25 Jul. 2024].

[13] EPA. U.s. environmental protection agency. [Online] Available at: https://www.epa.gov/ghgreporting/ghgrp-emissions-location. [Accessed: 15 Aug. 2024].

[14] U. E. P. A. (EPA). Greenhouse gas reporting program (ghgrp). [Online] Available at: https://www.epa.gov/ghgreporting. [Accessed: 15 Aug. 2024].

[15] ERCOT. Combined wind and solar. [Online] Available at: https://www.ercot.com/gridmktinfo/dashboards/combinedwindandsolar. [Accessed: 15 Aug. 2024].

[16] ERCOT. Item 5: Ceo board update. [Online] Available at: https://www.ercot.com/files/docs/2024/04/22/5%20CEO%20Update.pdf. [Accessed: 15 Aug. 2024].

[17] ERCOT. Load forecast. [Online] Available at: https://www.ercot.com/gridinfo/load/forecast. [Accessed: 15 Aug. 2024].

[18] ERCOT. Maps. [Online] Available at: https://www.ercot.com/news/mediakit/maps. [Accessed: 25 Jul. 2024].

[19] ERCOT. Report on existing and potential electric system constraints and needs. [Online] Available at: https://www.ercot.com/files/docs/2022/12/22/2022_Report_on_Existing_and_Potential_Electric_System_Constraints_and_Needs.pdf. [Accessed: 25 Jul. 2024].

[20] ERCOT. Report on existing and potential electric system constraints and needs. [Online] Available at: https://www.ercot.com/files/docs/2023/12/22/2023-Report-on-Existing-and-Potential-Electric-System-Constraints-and-Needs.pdf. [Accessed: 25 Jul. 2024].

[21] K. Gray. Carbon utilization and storage atlas (fourth edition).

[22] IEA. Co2 emissions in 2023. [Online] Available at: https://www.iea.org/reports/co2-emissions-in-2023. [Accessed: 15 Aug. 2024].

[23] IPCC. The numbers behind the science. in climate change 2014: Mitigation of climate change (cambridge univ. press, 2022). [Online] Available at: https://www.ipcc.ch/assessment-report/ar6/. [Accessed: 15 Jul. 2024].

[24] A. Jodry, R. Girard, P. H. A. Nóbrega, R. Molinier, and M.-D. E. A. Faris. Industrial hydrogen hub planning and operation with multi-scale optimisation. Journal of Cleaner Production, 426:138750, 2023.

[25] L. A. Kahlor, J. Yang, X. Li, W. Wang, H. C. Olson, and L. Atkinson. Environmental risk (and benefit) information seeking intentions: The case of carbon capture and storage in southeast texas. Environmental Communication, 14(4):555–572, 2020.

[26] H. Li, J. H. Panchal, and X. Du. Quantification model uncertainty of label-free machine learning for multidisciplinary systems analysis. In International Design Engineering Technical Conferences and Computers and Information in Engineering Conference, volume 87318, page V03BT03A045. American Society of Mechanical Engineers, 2023.

[27] H. Li, J. Rahman, and J. Zhang. Optimal planning of co-located wind energy and hydrogen plants: A techno-economic analysis. In Journal of Physics: Conference Series, volume 2265, page 042063. IOP Publishing, 2022.

[28] H. Li, J. Yin, and X. Du. Uncertainty quantification of physics-based label-free deep learning and probabilistic prediction of extreme events. In International Design Engineering Technical Conferences and Computers and Information in Engineering Conference, volume 86236, page V03BT03A001. American Society of Mechanical Engineers, 2022.

[29] H. Li and J. Zhang. Towards sustainable integration: Techno-economic analysis and future perspectives of co-located wind and hydrogen energy systems. Journal of Mechanical Design, 146(2), 2024.

[30] H. Liu, P. Were, Q. Li, Y. Gou, and Z. Hou. Worldwide status of ccus technologies and their development and challenges in china. Geofluids, 2017(1):6126505, 2017.

[31] Z. Liu, Z. Deng, S. J. Davis, and P. Ciais. Global carbon emissions in 2023. Nature Reviews Earth & Environment, 5(4):253–254, 2024.

[32] T. A. Meckel, A. P. Bump, S. D. Hovorka, and R. H. Trevino. Carbon capture, utilization, and storage hub development on the gulf coast. Greenhouse Gases: Science and Technology, 11(4):619–632, 2021.

[33] K. B. Medlock III and K. Miller. Carbon capture in texas: Comparative advantage in a low-carbon portfolio. Rice University's Baker Institute for Public Policy, 2020.

[34] K. B. Medlock III and K. Miller. Expanding carbon capture in texas. Baker Institute Center for Energy Studies, 2021.

[35] M. Meinshausen, J. Lewis, C. McGlade, J. Gütschow, Z. Nicholls, R. Burdon, L. Cozzi, and B. Hackmann. Realization of paris agreement pledges may limit warming just below 2 c. Nature, 604(7905):304–309, 2022.

[36] O. F. Noyan, M. M. Hasan, and N. Pala. A global review of the hydrogen energy eco-system. Energies, 16(3):1484, 2023.

[37] A. Products. Air products' u.s. gulf coast hydrogen network: Enhanced reliability from the world's largest hydrogen pipeline. [Online] Available at: https://microsites.airproducts.com/h2-pipeline/pdf/air-products-us-gulf-coast-hydrogen-network^datasheet.pdf. [Accessed: 15 Aug. 2024].

[38] J. Rand, N. Manderlink, W. Gorman, R. H. Wiser, J. Seel, J. M. Kemp, S. Jeong, and F. Kahrl. Queued up: 2024 edition, characteristics of power plants seeking transmission interconnection as of the end of 2023. 2024.

[39] C. R. Service. Pipeline transportation of hydrogen: Regulation, research, and policy. [Online] Available at: https://www.everycrsreport.com/files/2021-03-02_R46700_294547743ff4516b1d562f7c4dae166186f1833e.pdf. [Accessed: 15 Aug. 2024].

[40] P. Sizaire, B. Lin, and E. Gençer. A novel hydrogen supply chain optimization model–case study of texas and louisiana. International Journal of Hydrogen Energy, 78:401–420, 2024.

[41] S. D. Stephens-Romero, T. M. Brown, J. E. Kang, W. W. Recker, and G. S. Samuelsen. Systematic planning to optimize investments in hydrogen infrastructure deployment. International journal of hydrogen energy, 35(10):4652–4667, 2010.

[42] H. Tools. North american merchant hydrogen plant production capacities. [Online] Available at: https://h2tools.org/hyarc/hydrogen-data/merchant-hydrogen-plant-capacities-north-america. [Accessed: 15 Aug. 2024].

[43] V. Vijayakumar, A. Jenn, and J. Ogden. Modeling future hydrogen supply chains in the western united states under uncertainties: an optimization-based approach focusing on california as a hydrogen hub. Sustainable Energy & Fuels, 7(5):1223–1244, 2023.

[44] X. Yue, S. Pye, J. DeCarolis, F. G. Li, F. Rogan, and B. Ó. Gallachóir. A review of approaches to uncertainty assessment in energy system optimization models. Energy strategy reviews, 21:204–217, 2018.

[45] A. Zakaria, F. B. Ismail, M. H. Lipu, and M. A. Hannan. Uncertainty models for stochastic optimization in renewable energy applications. Renewable Energy, 145:1543–1571, 2020.